



1700MPa UHSS 3D Roll Bending a Pillar Reinforcement in the CFRP Side Frame for Ultimate Lightweight and Crash Safety

C. Gao¹(✉), G. L. Yuan², Y. F. Zhang², T. H. Li³, J. S. Zhang¹, Q. Yang¹, G. Feng¹, and H. Zhao¹

¹ Changan Global R&D Center, Changan Automobile Co., Ltd, Chongqing 400000, China
gaocong@changan.com.cn

² Vehicle Development Department, Changan New Energy Automobile Co., Ltd,
Chongqing 400000, China

³ School of Artificial Intelligence, Chongqing University of Technology, Chongqing 400000,
China

Abstract. With the tightening of energy consumption and emission regulations, automotive lightweight is more and more imperative. Herein, A-pillar upper reinforcement using 1700 MPa ultra-high strength steel (UHSS) 3D roll bending was firstly designed and applied to carbon fiber reinforced plastics (CFRP) side frame to achieve extreme lightweight and collision safety performance. The load extraction and subsystem model structure optimization methods were developed to solve the problems of large analysis model and low calculation efficiency in the traditional optimization iteration process. Finally, the application of 1700 MPa UHSS 3D-roll bending A-pillar upper reinforcement onto the CFRP side frame can reduce the weight by 19%, and improve the collision performance effectively.

Keywords: 3D roll bending · A pillar · CFRP · Automotive lightweight · Crash safety

1 Introduction

With the increase of car ownership in the world, a series of problems such as energy shortage and environmental pollution have become increasingly prominent. However, it is increasingly urgent for traditional fuel vehicles to meet the new fuel consumption regulations and the demand for the improvement of mileage of new energy vehicles. Vehicle safety and vehicle lightweight usher in a new round of development opportunities and tests. Vehicle lightweight can reduce vehicle quality, improve fuel efficiency and mileage. At the same time, automobile safety is also essential and the requirements are more and more strict.

Carbon fiber reinforced plastics (CFRP) is gradually replacing traditional metal materials due to its light weight, high strength, excellent damping, impact and fatigue resistance. Compared with the steel of the car body and chassis components, CFRP

components can reduce the weight by up to 50%, and its collision absorption capacity is 4 ~ 5 times higher than metal material, and CFRP components can be integrated design, which can greatly reduce the cost of assembly. In 2013, BMW i3 was launched, using a combination of CFRP body and aluminum alloy frame. Through modular design, the number of components of the car body was greatly reduced, and the weight reduction reached 30%, which is the first mass application of CFRP body in the automobile area. However, the low elongation at break (<3%) and complex processing technology of CFRP limited its application on the high deformation areas with complex structure, especially on the A pillar reinforcement.

3D roll bending of ultra-high strength steel (UHSS) is an important innovative technology in the field of UHSS forming in recent years. It can realize accurate die-free continuous bending of pipes, profiles and wires, especially for complex spatial shape bending members or complex bending members with continuous change of bending radius. Under the program control, the section die can realize 6 degrees of freedom motion (in which the z-direction displacement is the relative motion based on the work piece), and the special-shaped section straight profile can be continuously bent into a spatial geometry with continuous curvature change.

In this paper, the 3D roll bending A-pillar upper reinforcement (3D rolling A-pillar) was firstly designed and applied to the CFRP car body design for the first time to achieve the ultimate lightweight and collision safety performance simultaneously. The application of 3D roller tubes on the A-pillar upper side beams on carbon fiber vehicle bodies was systematically analyzed from the perspectives of material selection, structure and connection design, CAE simulation analysis and crash performance verification.

2 Material Properties and Structural Design

2.1 Material Properties

The materials of 3D rolling A-pillar are 1700MS and extruded profiles. The main manufacturers of ultra-high strength steel are SSAB and US steel in Sweden. The inner and the outer panel of the side frame was made of CFRP, of which the tensile strength was 1900 MPa. The 3D rolling A-pillar and the inner & outer panel of the side frame were connected by structural adhesive (Table 1).

Table 1. Material properties of 1700MS, CFRP and adhesive.

Component	Material	Density (g/cm ³)	Tensile strength (MPa)	Tensile modulus (GPa)
3D rolling A-pillar	MS1700	7.85	1700 ~ 2000	230
Inner & outer panel of the side frame	CFRP	1.55	1900	110
Structural adhesive	polyurethane	1.30	10	21

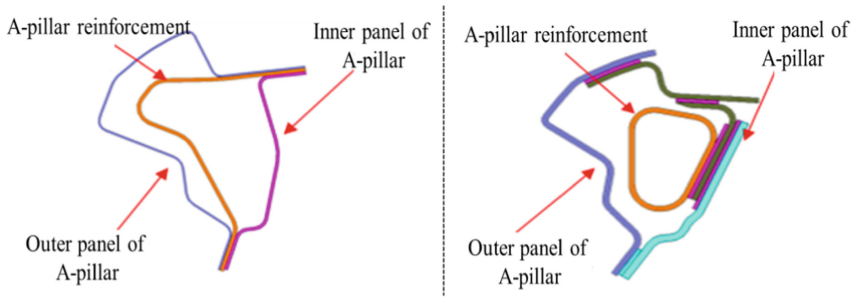


Fig. 1. Traditional structure and new designed structure of A-pillar.

2.2 Structural Design

The section structure of the A-pillar of the traditional car was composed of the side wall outer plate, the A-pillar upper reinforcement and the A-pillar upper inner plate. Mostly, the side wall outer plate and the A-pillar upper inner plate are steel plates, and the A-pillar upper reinforcement is hot-formed steel. The specific structure is shown in Fig. 1 for traditional structure and new designed structure. In this work, CFRP was combined with 3D rolling A-pillar, and structural adhesive was used to bond them together. The specific structure is shown in the following figure.

Using the closed structure advantage of 3D rolled pipe, the A-pillar cavity can be designed smaller on the premise of meeting the same performance, so as to achieve the purpose of reducing the obstacle angle of A-pillar. Compared with the traditional car, obstacle angle of A-pillar was reduced by 0.5 degrees.

2.3 Connection Design

3D rolling A-pillar was a closed structure, which cannot be connected with surrounding parts by traditional spot welding. Considering the progress of parts and welding performance, laser welding was adopted. The connection form of A-pillar was laser welding of A-pillar reinforcement and 3D rolled pipe, and the connection of A-pillar inner plate and 3D rolled pipe bolts, which increased the shear force and can absorb the assembly tolerance. The connection form of B-pillar was laser welding of B-pillar reinforcement and 3D roll bending parts, and laser welding of B-pillar inner plate and 3D roll bending parts. The connection form of C-pillar was laser welding between C-pillar connector and 3D roll bending part, and spot welding with the vehicle body. The connection process is shown in Fig. 2. And the side beam assembly on the A-pillar was connected with the inner & outer plate using the structural adhesive.

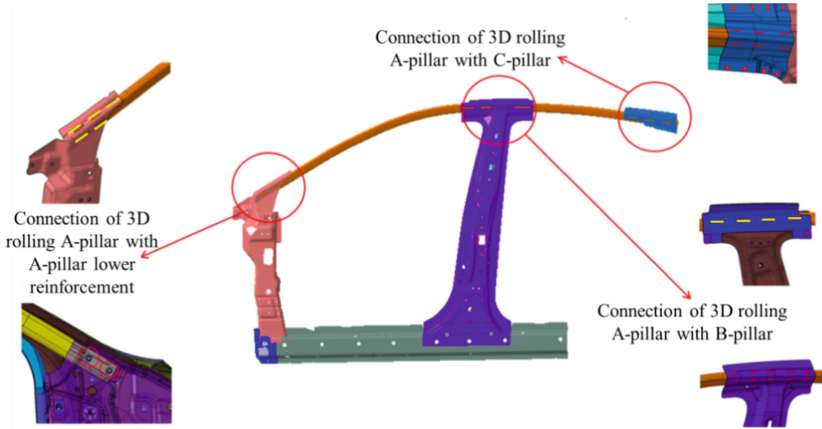


Fig. 2. The connection process of 3D rolling A-pillar assembly.

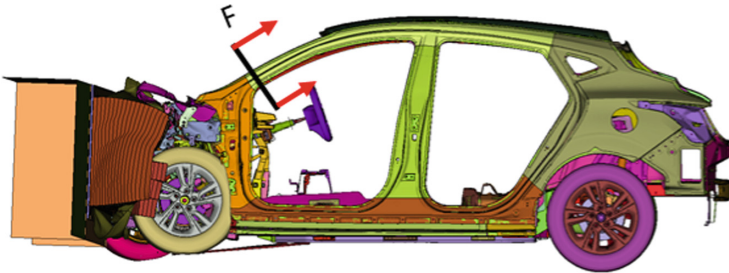


Fig. 3. ODB working condition deformation diagram of reference vehicle.

3 CAE Analysis

3.1 Load Extraction of A-Pillar Under Vehicle Working Condition

Among the three vehicle collision conditions of C-NCAP, ODB condition has the highest requirements for A-pillar structure, so the section force of A-pillar under this condition was extracted as the input load of subsystem model. The reference vehicle type can be selected according to the following principles: the same level, similar structure and equivalent curb weight of the whole vehicle. The section force was dynamic, which can be converted into an average constant force in the time domain and loaded on the subsystem. The conversion formula is as follows:

$$F_m = \frac{\int_0^T F(t)dt}{T} \quad (1)$$

in which, t is the ODB working condition analysis time of 120 ms. The ODB working condition deformation diagram and average section force of the reference vehicle is shown in Fig. 3 and Fig. 4.

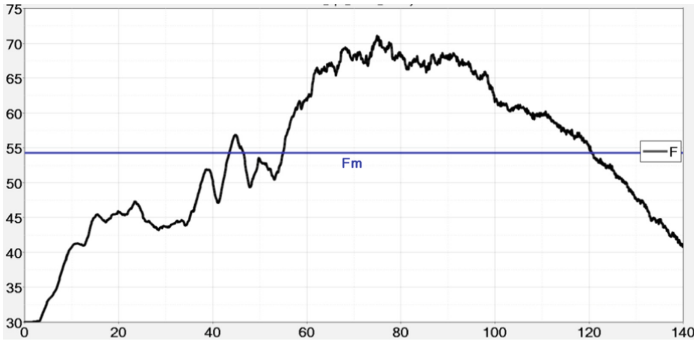


Fig. 4. Average section force of the reference vehicle.

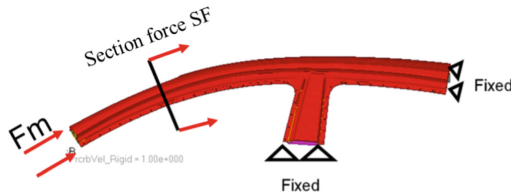


Fig. 5. A column system model.

3.2 Subsystem Model Establishment and Optimization Analysis

There are two problems in parametric analysis under the vehicle model: 1) the construction of vehicle parametric model is complex and time-consuming. 2) Parameter optimization simulation analysis requires a lot of iterations, and the calculation efficiency of vehicle working conditions is low and uneconomical. The efficiency of subsystem analysis and calculation can be greatly improved, but there are also two problems: 1) how to determine the boundary conditions of subsystem model to accurately reflect the working conditions of the whole vehicle. 2) How to select the evaluation index of subsystem model to reflect the crash performance of the whole vehicle.

A column system model is shown in Fig. 5. The reference vehicle system model unit and connection were consistent with the reference vehicle model, of which the unit size is 4 mm, $el_{form} = 2$, $nip = 5$. The solder joint is simulated by hexahedron element; between the welding point and each part through *contact_TIED_NODES_TO_Surf contact realizes connection. The load was the extracted average sectional force of A-pillar under ODB condition of reference vehicle. The lower end of B column and the rear end of a column were fixed and restrained. The evaluation index was the sectional force of a column of subsystem model. The greater the section force, the greater the load borne by the column. The smaller the deformation, the higher the strength, and the better the protection of passengers.

Compared with the reference vehicle system model, the changes of the design vehicle system model are as follows: 1) due to the reference vehicle model, the outer boundary of its inner surface and outer surface was relatively fixed. The inner and outer plates were designed with carbon fiber, and their thickness was increased, so the overlapping

Table 2. Preliminary parameters of the side frame.

Items	Parameters
Ply design of the outer panel	0/0/45/0/0/0/45/0/0
Ply design of the inner panel	0/0/-45/0/90/0/-45/0/0
L1	13 mm
L2	13 mm
L3	26 mm
L4	26 mm
Side angle α	0°
Thickness	2.2 mm

**Fig. 6.** A-pillar section of traditional car and new designed car.**Table 3.** Weight and maximum section force of the vehicle system.

Vehicle type	Weight of the subsystem model/kg	Maximum section force/kN
Reference car	7.18	63.9
Designed car	6.17	71.2

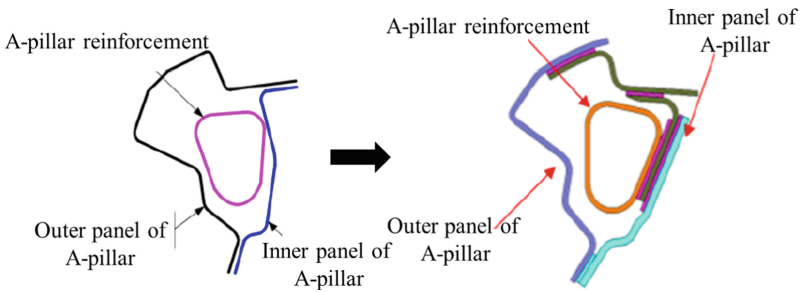
position of parts was adjusted; 2) The internal reinforcement was replaced by 3D roll elbow; 3) The parts were bonded.

The optimization parameters of the design car system model are the ply angle of CFRP of inner and outer plates, the side length and thickness of 3D roll elbow section. According to the principle that the section size was as large as possible and there are as many 0° paving layers as possible, the preliminary parameters are shown in Table 2.

The section of A-pillar of reference vehicle and design vehicle is shown in Fig. 6. After calculation, the weight and maximum section force of the vehicle system model designed after the initial parameters are shown in Table 3.

Table 4. Optimized parameters of the side frame.

Items	Parameters
Ply design of the outer panel	0/-45/0/45/0/45/0/-45/0
Ply design of the inner panel	0/45/0/-45/90/-45/0/45/0
L1	14 mm
L2	9 mm
L3	23 mm
L4	23 mm
Side angle α	25°
Thickness	2.0 mm

**Fig. 7.** The optimized section of 3D rolling A pillar.**Table 5.** Weight and maximum section force of the final design vehicle.

Vehicle type	Weight of the subsystem model/kg	Maximum section force/kN
Reference car	7.18	63.9
Designed car	5.82	71.5

The lightest weight of the subsystem model and the maximum section force was above the maximum section force of the reference vehicle are taken as the objectives and constraints of the iterative optimization of the subsystem model parameters. The parameters that meet the conditions are shown in Table 4.

The optimized section of the 3D rolling A pillar is shown in Fig. 7. Considering the machinability of parts, the number of parts and the overlapping relationship were further optimized. The subsystem model weight and maximum section force of the final design vehicle are shown in Table 5.

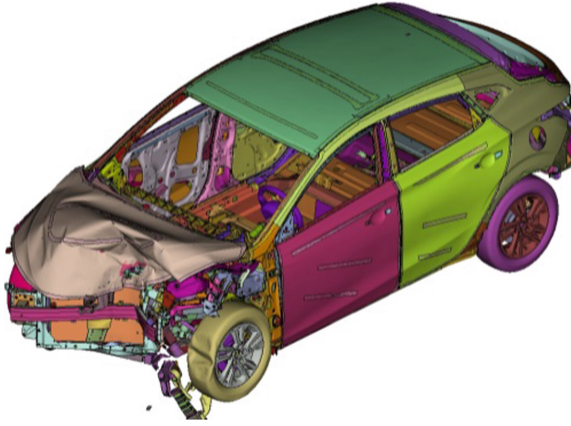


Fig. 8. Structural response of the whole vehicle under ODB conditions.

Table 6. Structural response parameters (simulation) of the whole vehicle under ODB conditions.

Items		Reference car	Designed car
Peak acceleration of B-pillar (g)	Left	42.2	31.23
Vehicle rebound moment (ms)	Left	94.8	95.99
Intrusion volume of the firewall (mm)	Firewall	102	102.6
	Driver's side footwell (Left)	68.2	102.6
Displacement of the accelerator pedal (mm)	X direction	47.2	31.67
	Z direction	21.5	15.81
Displacement of the brake pedal (mm)	X direction	69.1	85.27
	Z direction	24	40.18
Displacement of the steering column (mm)	X direction	28.2	22.16
	Y direction	15.3	14.71
	Z direction	-55	27.28
Intrusion volume of the left door frame (mm)	Upper hinge of door frame	23.6	9.51
	Lower hinge of door frame	22.3	19.28

3.3 Vehicle Model Simulation Analysis

The optimized A-pillar inner and outer plates and 3D roll bends were put into the vehicle model for simulation analysis. The results show that the structural response of the vehicle under ODB working conditions of this project reached the level of the reference vehicle and meet the requirements of collision safety. The structural response parameters of the whole vehicle under ODB conditions of the project were shown in Fig. 8 and Table 6.

By unifying the influencing factors such as the outer boundary, CFRP material parameters, ply parameters and changing the variables such as the section structure and material thickness of the 3D rolling A-pillar, the same performance goal was achieved. The contribution of 3D rolling A-pillar to weight and performance was greater, which can reduce the weight by 1.36 kg on the premise of meeting the same performance, and the structural response of the whole vehicle under ODB working condition reached the level of the reference vehicle.

4 ODB Crash Test

The results of the vehicle offset crash test showed that: 1) after the test, the A-pillar structure has no obvious deformation, and the structure was complete, meeting the design requirements; 2) The acceleration, deformation and other indicators of vehicle structure did not exceed the target requirements (Fig. 9 and Table 7).



Fig. 9. The vehicle performance after ODB Crash test.

Table 7. Structural response parameters (test) of the whole vehicle under ODB conditions.

Items		Reference car	Designed car
Peak acceleration of B-pillar (g)	Left	31.23	32.8
Vehicle rebound moment (ms)	Left	95.99	115
Intrusion volume of the firewall (mm)	Firewall	102.6	53
	Driver's side footwell (Left)	102.6	

(continued)

Table 7. (continued)

Items		Reference car	Designed car
Displacement of the accelerator pedal (mm)	X direction	31.67	36.9
	Z direction	15.81	12.9
Displacement of the brake pedal (mm)	X direction	85.27	44.1
	Z direction	40.18	12.3
Displacement of the steering column (mm)	X direction	22.16	-34.4
	Y direction	14.71	-5.7
	Z direction	27.28	-44.7
Intrusion volume of the left door frame (mm)	Upper hinge of door frame	9.51	9.3
	Lower hinge of door frame	19.28	10.7

5 Conclusion

A-pillar upper reinforcement using 1700 MPa ultra-high strength steel (UHSS) 3D roll bending was firstly designed and applied to carbon fiber reinforced plastics (CFRP) side frame to achieve extreme lightweight and collision safety performance. The load extraction and subsystem model structure optimization methods were developed to solve the problems of large analysis model and low calculation efficiency in the traditional optimization iteration process. Finally, the application of 1700 MPa UHSS 3D-roll bending A-pillar upper reinforcement onto the CFRP side frame can reduce the weight by 19%, and improve the collision performance effectively.

Acknowledgements. The research was funded by National Natural Science Foundation (U1909220, 62004020), Chongqing Key Projects of Technological Innovation and Application Development (cstc2021jscx-dxwtBX0022), National Key Research and Development Program of China (2016YFB01101703).

References

1. H. Yu, H. Zhao and F. Shi, Bending performance and reinforcement of rocker panel components with unidirectional carbon fiber composite, *Materials* **12**, 3164 (2019).
2. X. Pu, Q. Yang, S. Lan, S. Jia, B. Liu, Z. Li, Z. Wang and J. Zhang, A comparative study on comprehensive performance of 1800HS and 1500HS, *Advanced High Strength Steel and Press Hardening* **52**, (2020).

Open Access This chapter is licensed under the terms of the Creative Commons Attribution-NonCommercial 4.0 International License (<http://creativecommons.org/licenses/by-nc/4.0/>), which permits any noncommercial use, sharing, adaptation, distribution and reproduction in any medium or format, as long as you give appropriate credit to the original author(s) and the source, provide a link to the Creative Commons license and indicate if changes were made.

The images or other third party material in this chapter are included in the chapter's Creative Commons license, unless indicated otherwise in a credit line to the material. If material is not included in the chapter's Creative Commons license and your intended use is not permitted by statutory regulation or exceeds the permitted use, you will need to obtain permission directly from the copyright holder.

